frontiers in Water

ORIGINAL RESEARCH
published: 06 August 2021
doi: 10.3389/frwa.2021.706932

Groundwater Dominates Water Fluxes in a Headwater Catchment During Drought

Robin Kaule and Benjamin S. Gilfedder*

Limnological Station and Department of Hydrology, University of Bayreuth, Bayreuth, Germany

Headwaters make up a large part of the global stream length. They are also especially sensitive to droughts, which affect the stream's water balance, chemistry, and ecology. Climate change scenarios predict an increasing frequency of extreme weather events. For streams, rivers, and their catchments, this implies a higher intensity and frequency of severer droughts and floods. It is likely that during drought streams depend to a significant extent on groundwater to maintain flow. This study contributes to ongoing research on the effects of drought on headwater catchments and the role of groundwater in the water balance of these systems. Monthly Radon (^{222}Rn) measurements combined with mass balance calculations were used to quantify the spatial and temporal variability of groundwater influx to the Mähringsbach, a headwater catchment in northern Bavaria, Germany. Sampling was conducted in 2019 and 2020, a multi-year drought period, with 2019 being the seventh driest year since the start of records. Thus measurements covered a broad range of flow regimes (0.04 m^3 s^{-1} to ~ 3 m^3 s^{-1}). ^{222}Rn activities ranged between ~500 Bq m^{-3} and ~8,500 Bq m^{-3} in the headwater, while further downstream, the activities and variability in activities were lower (~500 Bq m^{-3} to ~2,000 Bq m^{-3}). Results from the ^{222}Rn mass balance showed that in the headwater reaches, the proportion of groundwater varied between 10 and 70 %, while further downstream, it ranged between only 0 and 30%. There was a clear negative correlation between river discharge and the proportion of groundwater inflow to the stream. Less than 10% of the total discharge was derived from groundwater during high flow conditions, while under low flow in the headwater reaches, it increased to 70%. We conclude that aquatic ecosystems in headwaters become increasingly dependent on groundwater during drought periods as a source of water. This dependency will increase in the summer months given current climate predictions. This knowledge should be used to develop, refine, and apply management strategies for streams and the important habitats located in stream sediments (hyporheic zone) under a changing climate.

Keywords: groundwater, drought, radon, climate change, headwater, natural tracer

OPEN ACCESS

Edited by:
Sabarathinam Chidambaram, Kuwait Institute for Scientific Research, Kuwait

Reviewed by:
Asghar Azizian, Imam Khomeini International University, Iran
Leilei Min, Institute of Genetics and Developmental Biology (CAS), China

****Correspondence:***
Robin Kaule
robin1.kaule@uni-bayreuth.de

Specialty section:
This article was submitted to Water and Critical Zone, a section of the journal Frontiers in Water

Received: *08 May 2021*
Accepted: *09 July 2021*
Published: *06 August 2021*

Citation:
Kaule R and Gilfedder BS (2021) Groundwater Dominates Water Fluxes in a Headwater Catchment During Drought. Front. Water 3:706932. doi: 10.3389/frwa.2021.706932

INTRODUCTION

Headwater streams make up nearly 90% of the global stream system length (Downing, 2012; Allen et al., 2018; Ward et al., 2020). They are crucial for water quantity and quality downstream (Alexander et al., 2007). Headwaters are essential sources of high-quality water, diluting nutrient and other contaminant and sediment inputs, thus influencing habitat quality for aquatic organisms (Gomi et al., 2002). As such, they are a vital feature of aquatic ecosystems. They are also essential for public water supply. Spatial and temporal variations of hydrological, biological, and geomorphological processes in headwater systems strongly influence the dynamics of downstream aquatic ecosystems, channel conditions, and material transport (Gomi et al., 2002). Harder et al. (2015) found that glacier-fed headwaters show remarkable resilience toward such changes. However, small fluvial aquatic ecosystems without water storage reserves (e.g., snowpack or glaciers) are especially threatened by effects of climate change (e.g., shifted precipitation patterns, the distribution between rain and snow, and more frequent and severe droughts) (Bennett et al., 2012).

The IPCC (2014, 2018) predicts an increase in weather extremes as the climate changes. This is likely to lead to an increasing frequency and magnitude of floods and droughts in countries such as Germany (Huang et al., 2015). Blöschl et al. (2017) analyzed shifts in the timing of floods in Europe. They found that if the current trend of flooding shifting to earlier in the year continues, considerable ecologic consequences may arise as ecosystems are not adapted to the new flood regime. The alternating occurrence of long periods of drought followed by heavy precipitation events described by Huang et al. (2015) will likely result in an increase of floods that are independent of season but a decreased water availability in summer (Zerbisch et al., 2005).

While flood events have received considerable attention due to their destructive impacts on society and ecosystems (van Loon, 2013), droughts and their effects have received comparatively little attention to date, especially in Europe, which is traditionally seen as having sufficient water. The need for a deeper understanding of the causes and effects of droughts in Europe has been highlighted by van Loon (2013).

Intact Headwater catchments in forested low mountain ranges are relatively cold due to their altitude and shading by trees. Luce et al. (2014) have suggested that cold streams are less sensitive to increases in air temperature but may be threatened by secondary impacts of climate change, such as decreased summer flows and reduced groundwater recharge. Modeling by Kingston and Taylor (2010) suggested that climate change will increasingly alter seasonal river discharge and river water sources. In Kingston and Taylor (2010), the groundwater inflow decreased in summer due to increased evapotranspiration and less groundwater recharge, and groundwater contribution to river discharge decreased (Kingston and Taylor, 2010). Zhou et al. (2014) have reviewed the influence climate change has on groundwater-surface water interaction due to rising evapotranspiration rates, changes in the spatial distribution of precipitation, and how rising water temperature influences flow volume during peak discharge and base flow. They concluded that groundwater-surface water interactions will be altered by climate change, the effect on rivers ranging from reach scales (e.g., distribution of interstitial pollutants and change in function and structure of hyporheic communities) to whole catchment scale (e.g., water quality and bulk hydrological exchange).

The hyporheic zone (the interface between groundwater and stream water) is an essential habitat for a diverse range of species (Boulton et al., 1998; Hancock et al., 2005; Kawanishi et al., 2013). Hyporheic exchange and groundwater up-welling areas are vital for fish embryos and invertebrates (Sternecker et al., 2013) by providing an oxygen-rich and temperature buffered habitat (Cardenas et al., 2016; Kaufman et al., 2017). The hyporheic zone is also a refuge for invertebrates during floods, drought, and from predation (Boulton et al., 1998). These organisms often form the base of the food chain and are crucial for the entire ecology of the stream.

During drought, groundwater can become an important or even the sole water source for streams (Cartwright and Gilfedder, 2015). Groundwater flux can vary temporally and spatially, and some reaches receive groundwater discharge preferentially (Schubert et al., 2020, Cook, 2013, Atkinson et al., 2015). Since the thermal and chemical properties differ significantly between groundwater and surface waters, understanding groundwater-stream interaction is essential for understanding fundamental shifts in stream chemistry, aquatic ecosystem structure, composition, and health, especially as climate changes. For example, Boulton et al. (1998) state in their review that up-welling water can promote hot spots of biological production in rivers. In contrast, Malcolm et al. (2003) state that upwelling groundwater decreases the survival rate of salmonid eggs due to its low dissolved oxygen levels and chemically reduced properties. This shows that both the flux and chemical composition of the groundwater is a controlling factor for the hyporheic habitat.

As Zhou et al. (2014) have shown, more work is needed to quantify the effect climate-related factors have on water exchange rates between ground and surface water. There are various approaches to quantify groundwater-surface water interactions, including various tracers and models (Hatch et al., 2006; Keery et al., 2007; Constantz, 2008; Cartwright et al., 2011; Bartsch et al., 2014; Anibas et al., 2017; Gilfedder et al., 2019). A detailed overview of these methods can be found in Cook (2013).

In general, the higher the concentration gradient of the tracer between ground- and surface water, the more sensitive and robust the method is. Radon (^{222}Rn) is a particularly sensitive tracer due to the large contrast in groundwater and surface water activities. This disequilibrium is maintained by radioactive decay and loss to the atmosphere in surface water and production in the aquifer. Cook (2013) found ^{222}Rn to be the most suitable tracer for groundwater fluxes because it can detect rates as low as ∼2 mm/day. ^{222}Rn has been applied successfully as a tracer in many studies to investigate groundwater-surface-water exchange and the residence time of stream water in the hyporheic zone (Lamontagne and Cook, 2007; Bourke et al., 2014; Pittroff et al., 2017). There are three naturally occurring radioisotopes: ^{219}Rn, ^{220}Rn, and ^{222}Rn. Whereas, ^{219}Rn and ^{220}Rn have short half-lives

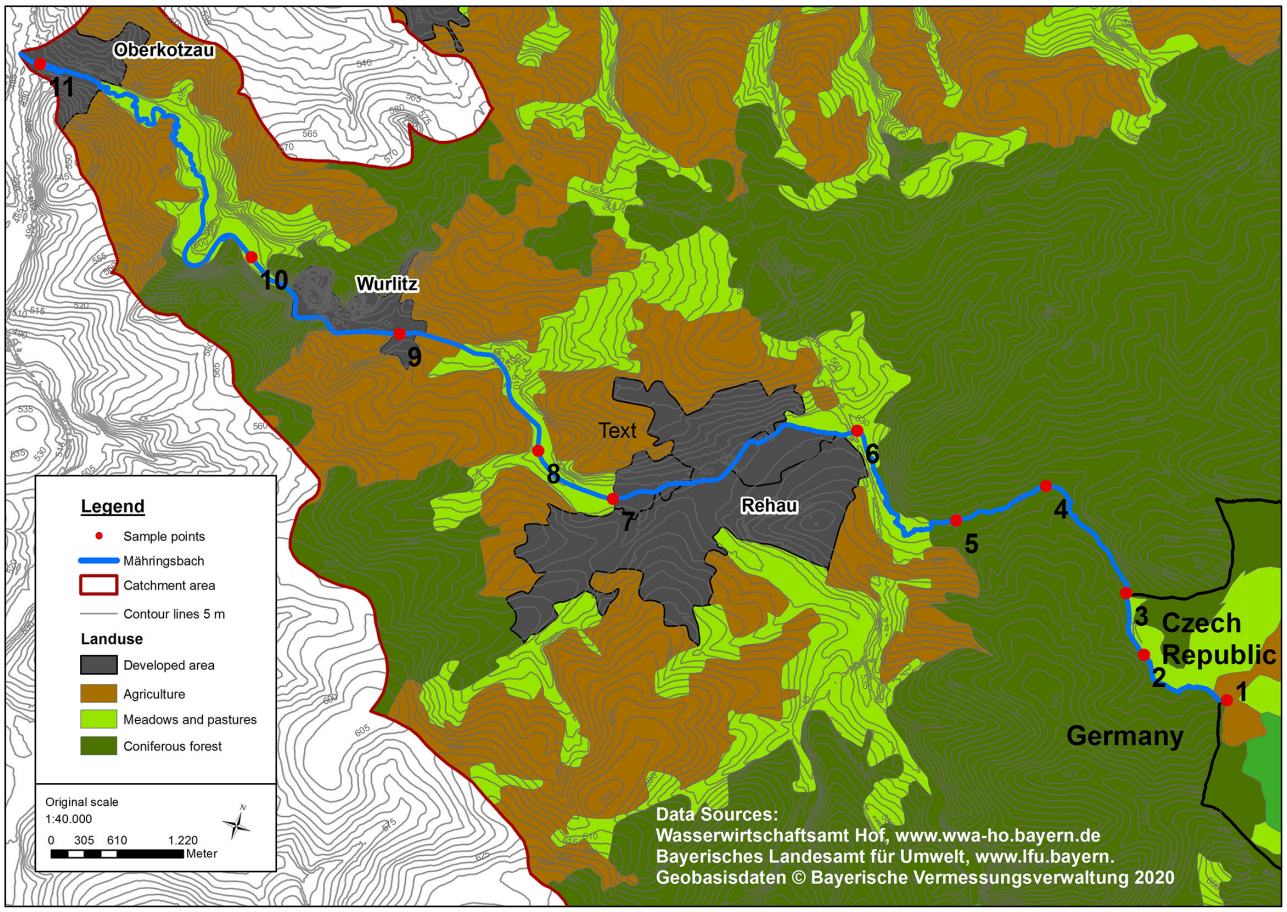

FIGURE 1 | Land-use and topographic map of the Mähringsbach catchment with sampling sites.

(<1 min), ^{222}Rn has a half-live of ~3.82 days. ^{222}Rn is a noble gas and is part of the ^{238}U decay chain. The only ^{222}Rn sink in the saturated zone is radioactive decay. Emission and decay of ^{222}Rn in the aquifer result in a steady-state activity that defines the groundwater end-member. Stream water ^{222}Rn activities are lower due to degassing to the atmosphere as well as decay. However, hyporheic exchange can increase ^{222}Rn concentrations in stream water as water flowing through the hyporheic zone comes in contact with sediments containing ^{226}Ra (Lamontagne and Cook, 2007).

This work focuses on elucidating hydrological resilience vs. sensitivity of headwater catchments during drought in 2019 and 2020. We investigate how drought affects groundwater fluxes along a headwater stream and the proportion of groundwater composing stream discharge. 2019 was the seventh driest year since 1910, when records began, while 2020 had approximately average precipitation. We aim to contribute to a better understanding of how regime shifts due to drought impact headwater ecosystems (e.g., habitat changes) by analyzing spatial shifts of gaining reaches, including an assessment of groundwater inflow variability and the identification of shifting groundwater inflow hotspots along the channel of the stream.

MATERIALS AND METHODS

Study Area

The Mähringsbach catchment is located in southeast Germany, with the upper parts of the catchment in the Fichtel Mountains. The Mähringsbach is a tributary of the Höllbach, which flows into the Schwesnitz. The Schwesnitz finally joins with the Sächsische Saale, a second-order river that flows into the Elbe. For simplicity, we refer to the entire 16.3 km from the spring to the confluence with the Sächsische Saale as "Mähringsbach." The catchment area is 102 km^2. The stream originates from an elevation of about 580 m in a groundwater-fed peaty fen located at the German-Czech border. The land use in the catchment consists of coniferous forests, grassland, cropland, and small settlements, including some industrial areas (**Figure 1**). The headwater flows predominantly through coniferous forests and continues through cultivated land before joining the Saale. The first half of the stream runs through a phycode slate formation. The geology of the catchment downstream of Rehau is much more diverse, containing greywacke, serpentinite, phyllite, amphibolite series, and paragneiss. The aquifer is a crystalline cleft aquifer with a small storage capacity (Bayerisches Landesamt für Umwelt,

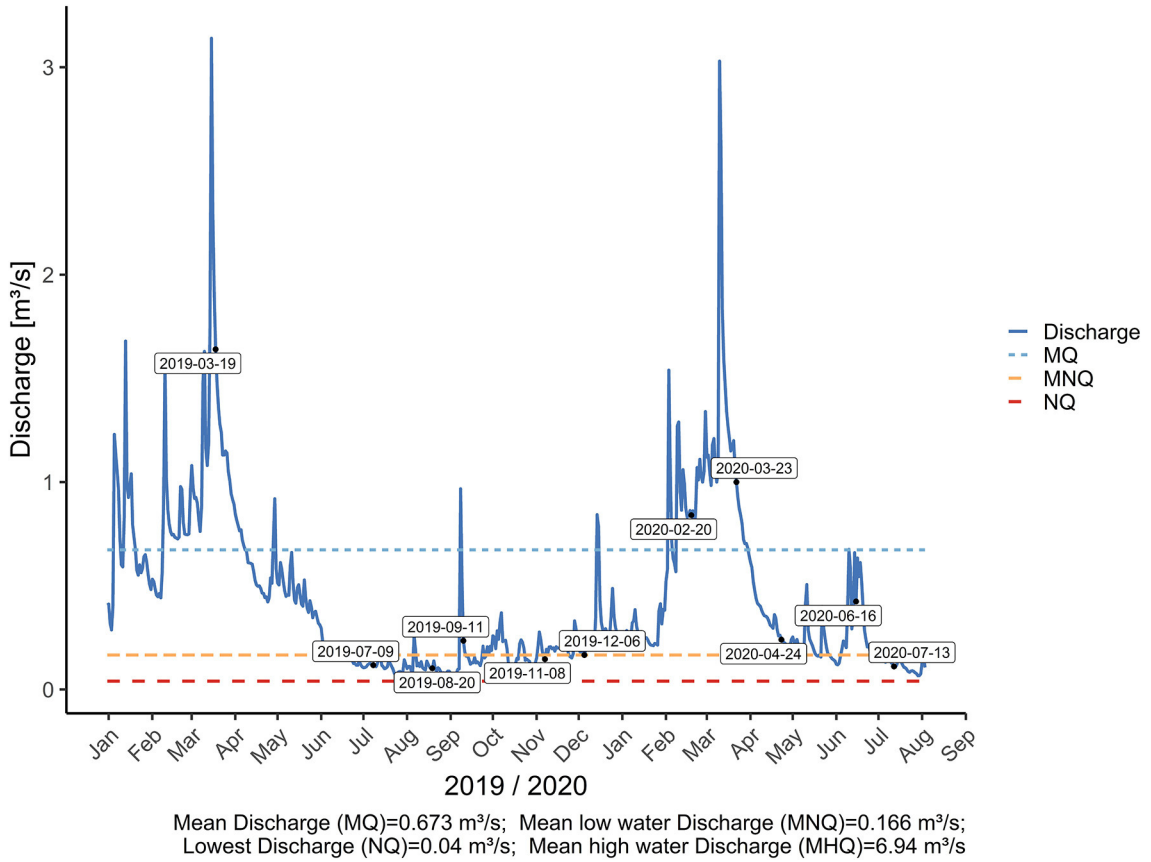

FIGURE 2 | Discharge and long-term discharge characteristics of the Mähringsbach at the water gauge Rehau. The blue dashed line shows the long-term average discharge at the gauge. The long-term low flow average is indicated by the orange dashed line. The red dashed line shows the long-term lowest discharge (lowest value of the last 30 years).

2017). The mean annual precipitation is 740 mm, and the mean annual temperature is 7.3°C (1991–2020; DWD weather station ID 4548 (Selb); Data obtained from the climate data center of the German Meteorological Society (2021).

The Mähringsbach is one of the last habitats for the severely endangered freshwater pearl mussel (*Margaritifera margaritifera*) in southeast Germany. Freshwater mussels s are considered the most endangered group of animals, and the freshwater pearl mussel is considered one of the most endangered freshwater mussels worldwide (Geist, 2010). Since 1859, over 50% of the freshwater pearl mussel's population and likely over 90% of the individual mussels have been lost due to habitat destruction (Denic and Geist, 2017). Temporal variation of groundwater-surface water interactions plays an essential role in their life cycle since the young mussels reside in the hyporheic zone for 5 years before staying partially buried in the sediment as adult mussels (Geist, 2010).

Sampling

Measurements were conducted at eleven sites (**Figure 1**) in the Mähringsbach between March 2019 and July 2020. Eleven sampling campaigns were conducted during all sessions to capture the yearly variability in discharge and groundwater inflow (**Figure 2**). The hydrological regime in the Mähringsbach represents the typical regime in central European streams, with higher flows in winter and spring and lower flows in summer and autumn. These patterns were also present during the sampling period (**Figure 2**). However, measurements were conducted during a multi-year drought. According to precipitation data obtained from the German Meteorological Society (DWD, 2021) 2018 was the second (508 mm) driest year since records started in 1910, while 2019 was the seventh driest year (550 mm) (**Table 1**). The year 2020 was the first year in 3 years with approximately average precipitation (752 mm). **Table 1** shows the yearly and seasonal deviations in precipitation from the reference time period (1981–2010). The mean discharge of the Mähringsbach at the discharge gauge Rehau [gauge number 56122008 (Bayerisches Landesamt für Umwelt, 2021)] is 0.7 m^3 s^{-1}. The mean low water discharge is 0.2 m^3 s^{-1}, and the mean high water discharge is 7.0 m^3 s^{-1}. The Precipitation deficit of the years 2018 and 2019 and the number of Measurements with discharge close to or even under the mean low water discharge (**Table 2**, **Figure 2**) clearly show the drought conditions during 2018 and 2019.

TABLE 1 | Precipitation data for the reference period (1981–2010) and the seasons of 2018, 2019, and 2020 from the DWD weather station ID 4548 (Data obtained from the climate data center of the German Meteorological Society (DWD, 2021)).

	$P_{1981\text{-}2010}$ [mm]	P_{2018} [mm]	P_{2019} [mm]	P_{2020} [mm]
Winter	196	180 (−8%)	132 (−33%)	165 (−16%)
Spring	167	127 (−24%)	133 (−20%)	104 (−38%)
Summer	249	111 (−55%)	95* (−62%)	258 (+4%)
Autum	189	90 (−52%)	190 (+0.4%)	225* (+19%)
Yearly	786	508 (−25%)	548 (−30%)	752 (−4%)

*Data with * contain missing values.*

TABLE 2 | Summary of the campaigns divided into three groups.

Group	Season	Date	Discharge gauge (daily mean in $m^3\ s^{-1}$)	Average ^{222}Rn upstream in Bq m^{-3}	Average ^{222}Rn downstream in Bq m^{-3}
1	Summer	2019-07-09	0.117	5,354	860
1	Autumn	2019-11-08	0.146	2,477	1,056
1	Summer	2020-07-13	0.111	3,448	774
2	Autumn	2019-09-11	0.235	3,816	1,083
2	Winter	2019-12-06	0.166	2,335	813
2	Spring	2020-04-24	0.240	2,519	984
2	Summer	2020-06-16	0.424	2,099	655
3	Autumn	2019-03-19	1.64	2,681	1,548
3	Winter	2020-02-20	0.84	2,101	1,271
3	Spring	2020-03-23	1.00	2,300	944

*The discharge was taken from the gauge in Rehau. The average ^{222}Rn activity upstream is calculated from the measurement points from the first site to the city of Rehau. Downstream from the points between Rehau and Oberkotzau (see **Figure 1**).*

The measurements from August 11, 2019, were excluded from the data set because groundwater was pumped into the stream to prevent it from falling dry and damaging the pearl mussel population. This alters the ^{222}Rn signature of the river water, leading to difficulties in distinguishing between ground and surface water sources. The discharge values from the Rehau gauge are only used to describe and compare the flow regimes. For all further calculations, the measured discharge at the time and location of the ^{222}Rn sampling was used.

The 11 sampling sites divide the stream into ten sections called reaches. In addition to stream samples, each of the major tributaries were also sampled during each campaign. Each reach is approximately 1.6 km long, ranging from 0.5 to 3.9 km. All samples were taken within 10 h of the first sample. Sample sites were located in all four land-use types (**Figure 1**). The discharge of the main channel and tributaries were measured at all sampling points with an electromagnetic current meter (SEBA Hydrometrie GmbH FlowSens) and the channel geometry using the 2-point-measurement of Kreps (1954).

For the ^{222}Rn measurements of the stream and tributaries, water samples were collected in one-liter plastic bottles. Each sample was filled and closed underwater in the middle of the stream to avoid degassing of ^{222}Rn and to ensure a representative water sample. River depth and width were measured at each site.

The ^{222}Rn groundwater end-member activity was estimated differently for the headwater and the downstream parts of the steam. For the headwater (first 5.3 km), we took sediment samples for incubation experiments similar to Corbett et al. (2006). Sediment samples from the stream bed were taken from sampling points two, four, and six. This was primarily done to incorporate potential heterogeneity in the groundwater end-member (Cook et al., 2008). These samples were taken from 10 to 20 cm depth directly from the stream bed using a spade and were incubated with stream water for 8 weeks in gas-tight four-liter glass containers. Samples (20 ml) were extracted from the incubation bottles with a mini-piezometer and measured immediately, as described below. Incubation experiments have the major benefit that many samples can be taken without installing piezometers into the stream bed or riparian zone. It also allows a much higher spatial resolution of the groundwater end-member than would otherwise be possible.

We used water samples from a single shallow groundwater well (10 cm screen, 120 cm below ground surface level) close to point six in the downstream part of the catchment. Samples were pumped from the piezometer and purged at least three times before samples were taken. Each sample was filled into one-liter bottles and bottom filled until overflowing to avoid degassing.

Radon Measurement

^{222}Rn was measured using a Durridge Rad7 (large dome, large detector) radon in air detector. We used a closed air loop approach to measure ^{222}Rn activity in water samples similar to the measurement described by Lee and Kim (2006). Each one-liter sample was purged for 5 min with ambient air and then counted three times for 60 min, and the averaged value was used for further calculations. Due to <12 h between sampling and measurement, no correction for radioactive decay was applied. The ^{222}Rn activities are expressed in Bq m^{-3} water. Similar approaches have been used by Frei et al. (2019), Pittroff et al. (2017), and Unland et al. (2013). The 20 ml samples were measured in the laboratory after purging the Rad7 with Nitrogen. This reduces ^{222}Rn in the ambient laboratory air from contaminating the sample, which is essential at low counting rates. Samples were counted two times for 60 min.

Analysis With FINIFLUX

Groundwater flux to the Mähringsbach was calculated using the mass-balance approach implemented in the FINIFLUX model developed by Frei and Gilfedder (2015). FINIFLUX solves the stream ^{222}Rn mass-balance equation (Equation 1) at the reach scale. A Petrov-Galerkin Finite Element scheme based on on-site radon measurement is used to calculate groundwater discharge to each reach between two sample points.

$$Q\frac{\delta c}{\delta x} = I(c_{gw} - c) - kwc - dw\lambda c + \alpha_1 - \alpha_2 c + \frac{Q_r}{R_L}(c_{trib} - c) \quad (1)$$

where Q $[L^3T^{-1}]$ is the stream discharge, c and $c_{gw}[ML^{-3}]$ are ^{222}Rn concentration in the stream- and groundwater respectively, x $[L]$ as 1-D stream length, I $[L^2T^{-1}]$ is the groundwater inflow rate, k $[LT^{-1}]$ is the degassing coefficient, w $[L]$ ^{222}Rn stream width, d $[L]$ is mean stream depth, λ $[T^{-1}]$ is the decay constant of ^{222}Rn, Q_r $[L^3T^{-1}]$ is the inflow from tributaries, R_L $[L]$ ^{222}Rn is the inflow length and c_{trib} $[ML^{-3}]$ is the tributary ^{222}Rn concentration. α_1 $[ML^{-1}T^{-1}]$ and α_2 $[L^{T-1}]$ represent the reach-specific loss and enrichment of ^{222}Rn in the hyporheic zone and are calculated using an exponential residence time distribution model. Frei et al. (2019) and Pittroff et al. (2017) describe α_1 and α_2 in more detail. The degassing coefficient k was calculated using an empirical equation from O'Connor and Dobbins (1958), modified to SI units by Mullinger et al. (2009) and Cartwright et al. (2011) (Equation 2).

$$k_{Rn} = 9.301 \times 10^{-3} \frac{v^{0.5}}{d^{1.5}} \quad (2)$$

Further description of the FINIFLUX model can be found in Frei and Gilfedder (2015) and Frei et al. (2019). The model assumes steady-state conditions and neglects evaporation (Frei and Gilfedder, 2015). Fitting and optimization of the model to the measured ^{222}Rn activities were executed with BeoPest (Doherty et al., 2010).

RESULTS

Radon Activities and Discharge

Measurements were made eleven times from March 2019 to July 2020. The measurement results were divided into three groups based on their discharge values (**Figure 2**). Group 1 contains all measurements with discharge values below average low water discharge. Group 2 includes the values between average low water discharge and average discharge, and group 3 includes the values above average discharge. **Figure 3** shows the development of the discharge and radon activities for the three groups in the Mähringsbach catchment during 2019 and 2020.

In the headwater (defined as the forested area until the stream reaches the city of Rehau, ∼5.3 km from the spring area), we measured radon activities ranging from 560 to 7,970 Bq m^{-3} for group 1, 430 to 8,670 Bq m^{-3} for group 2, and 880 to 5,830 Bq m^{-3} for group 3. This shows that approximately the entire measuring range is present in all three groups during the sampling period. The upstream stream sections generally show decreasing radon activities with increasing discharge (**Table 2**).

The end-member ^{222}Rn activities from the incubation experiments were 90,550 Bq m^{-3} for the first 1.5 km, 131,660 Bq m^{-3} for the next 2.2 km, and 90,270 Bq m^{-3} for the last 1.6 km of the headwater.

Downstream (defined from the city of Rehau to the last measuring point), radon activities ranged between 10 and 1,550 Bq m^{-3} in group 1, 370, and 1,500 Bq m^{-3} in group 2 and 520 to 2,000 Bq m^{-3} in group 3. This shows that only the lower third of the measurement range is present in the lower stream section. Moreover, downstream, group 3 has the highest ^{222}Rn activities, while upstream, the highest ^{222}Rn activities were observed in groups 1 and 2 (**Figure 3**, **Table 2**). The sample obtained from the piezometer used for the end-member downstream had a ^{222}Rn activity of 56,000 Bq m^{-3}.

Temporal and Spatial Groundwater Inflow Rate

The fit between measured and modeled ^{222}Rn values was used to indicate the quality of the modeled groundwater fluxes. As an example, for two contrasting campaigns, the model fits and groundwater fluxes of measurements from the highest (2019-03-19) and lowest (13-07-2020) discharge are shown in **Figure 4**.

Figure 5A shows the groundwater inflow expressed in m^3 d^{-1} m^{-1}. The mean values illustrate the spatial distribution of groundwater inflow for each reach over the measurement period. Along the Mähringsbach, groundwater inflow rates display a pattern with two clear peaks and two points with low groundwater discharge rates. Groundwater discharge above 0.2 m^3 d^{-1} m was observed in reaches 1, 2, and 9. These reaches are consistently the most influenced by groundwater inflow and show values between <0.1 and 0.6 m^3 d^{-1} m^{-1}.

In contrast, the reaches 3, 5, 6, 12, and 13 have low average inflow rates (below 0.2 m^3 d^{-1} m^{-1}) and displayed very low temporal variance (between near 0 and 0.2 m^3 d^{-1} m^{-1}). Reaches 8 and 11 are somewhat of an exception with low average groundwater inflow rates but high maximum values (0.4 m^3 d^{-1} m^{-1} for reach 8 and 0.5 m^3 d^{-1} m^{-1} for reach 11), indicating possible shifts of inflow hotspots.

Groundwater Surface Water Ratio

Groundwater inflow depended strongly on discharge. In the following, we calculate groundwater as a percentage of total discharge (equation 3). Here I is the groundwater flux, and Q is the discharge in each reach:

$$\textit{Groundwater flux in } \% = \frac{\sum_{i=1}^{n} I_i}{Q_i} \times 100 \quad (3)$$

Figure 6A shows the cumulative groundwater flux as a percentage of the total reach discharge. Overall, we observed a declining proportion of groundwater in reach discharge along the stream, starting with the highest groundwater proportion in reach 1. The declining trend is continued until reach 8. After this, values tend to stagnate at a low level (∼5% of discharge). The variance of the proportion of discharge composed of groundwater is largest in reaches 1 to 6 and highest in reaches 1 to 3. In the reaches, 8 to 13, the variance remains at a constant low level.

The proportion of groundwater and discharge show a rapidly declining relationship with stream length, with the highest values in the headwaters (**Figure 6B**). For group 1, we found stream water was composed of up to 70% groundwater, but this was only observed in the uppermost reaches. Downstream we found stream water was composed of maximum 20% groundwater. In group 2, groundwater made up to 50% of the stream water in the headwater. Downstream groundwater contribution was <15% of the discharge. Group 3 showed groundwater portions of around 10% or less along

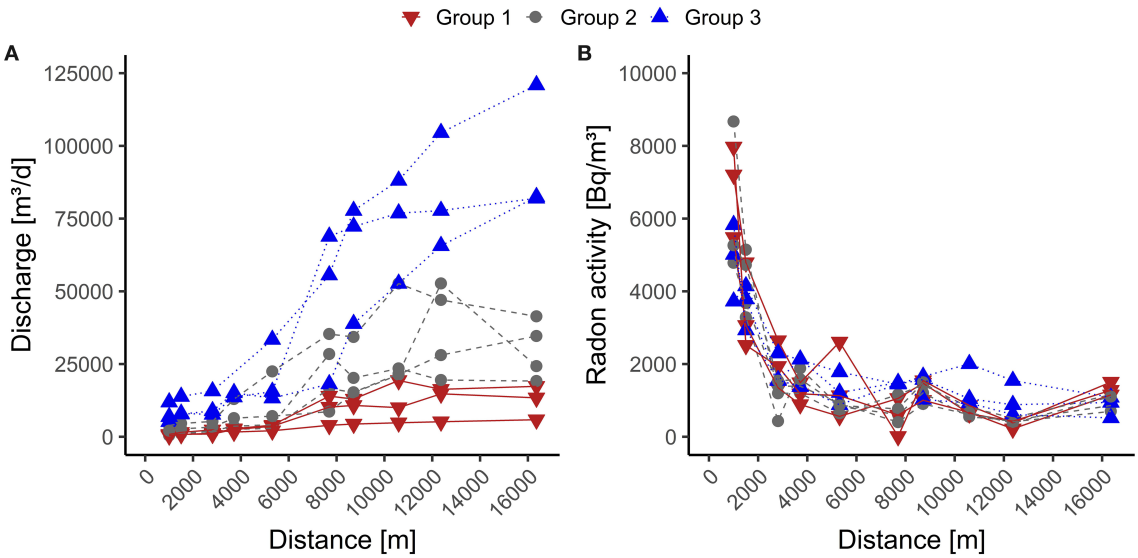

FIGURE 3 | Radon activity and discharge along the stream, separated by group 1 (discharge below average low water discharge), group 2 (discharge between average low water discharge and average discharge), and group 3 (discharge above-average discharge. **(A)** shows the change of discharge along the stream. **(B)** illustrate the change of ^{222}Rn activity along the stream.

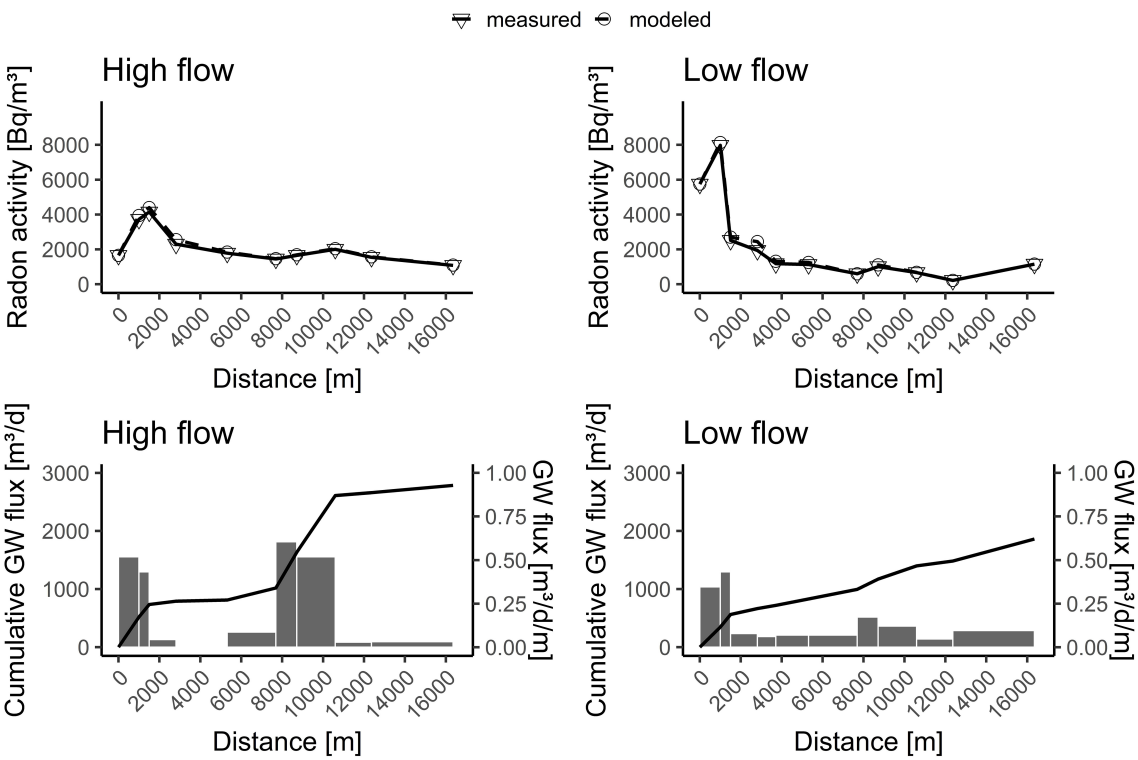

FIGURE 4 | Model fits and groundwater fluxes for two selected sampling campaigns. High flow regime March 19, 2019 (highest discharge); Low Flow regime July 13, 2020 (lowest discharge).

the whole stream length. In summary, our measurements of groundwater fluxes and their contribution to stream discharge indicate a positive correlation between groundwater inflow and stream discharge. However, the percentage of groundwater in the stream is negatively correlated to increasing discharge values.

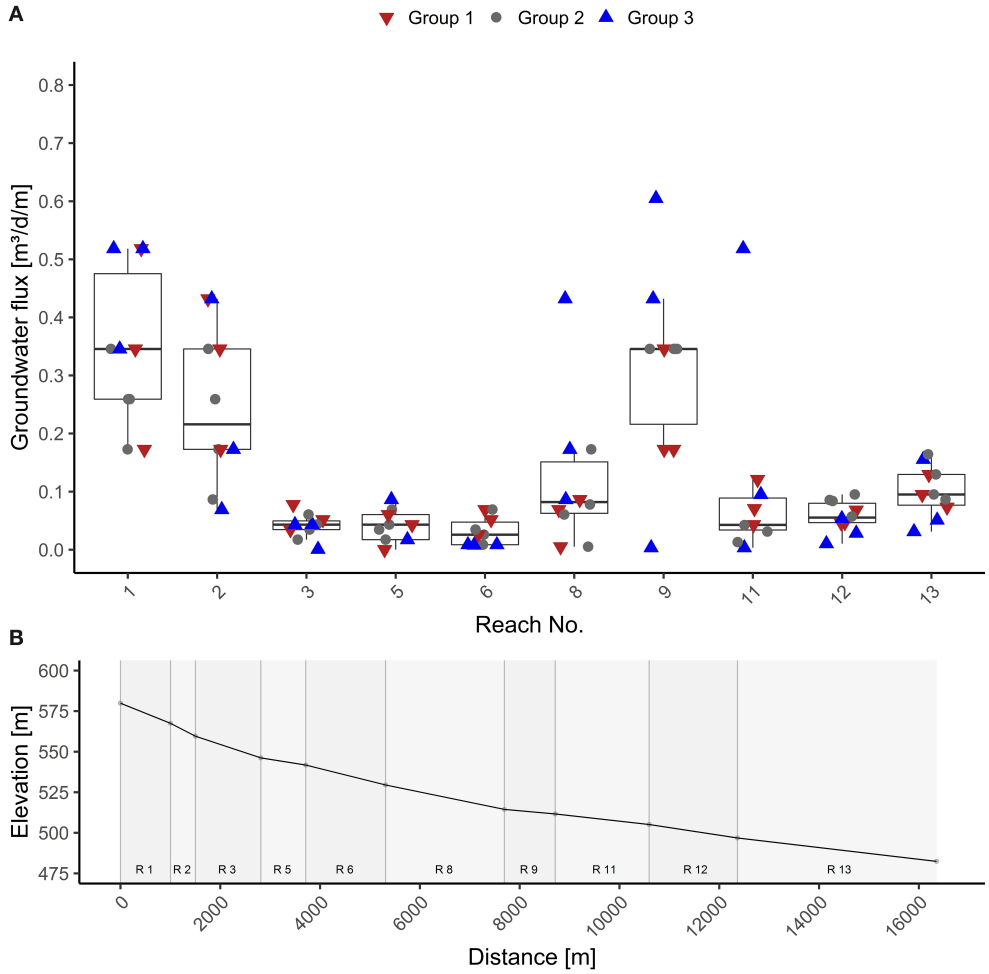

FIGURE 5 | Above **(A)** Variance of groundwater inflow in $m^3\ d^{-1}\ m^{-1}$ through the measurement period for each reach. Below **(B)** Elevation of the measurement points along the stream.

DISCUSSION

In this study, ^{222}Rn was measured over 16 months and used to quantify groundwater fluxes by mass balance. The groundwater inflow and the proportion of groundwater in the discharge along the Mähringsbach stream showed significant spatial and temporal patterns. While groundwater flux was high during times of high discharge, groundwater was a more significant proportion of streamflow during low flow conditions.

Constraints

Radon has been applied as a tracer for groundwater inflow in several studies from various continents, climate zones, and environments ranging from creeks to oceans and from arid to Humid climates (Burnett and Dulaiova, 2006; Cartwright et al., 2011; Bourke et al., 2014; Cranswick et al., 2014; Frei and Gilfedder, 2015; Frei et al., 2019). Atkinson et al. (2015) compared the groundwater flux obtained from ^{222}Rn data to two different tracers (Cl^- and ^{3}H) and found comparable (~20 %) results. Similarly, McCallum et al. (2012) combined tracers with sequential flow gauging and found that tracers provide information about the gross groundwater fluxes, while flow gauging can only measure net groundwater inflow. Although ^{222}Rn is becoming an increasingly used tracer for groundwater-surface water interactions, there are some challenges when ^{222}Rn is used quantitively. The most significant uncertainty is the groundwater end-member activity. Studies have shown that ^{222}Rn end-member activity can vary by an order of magnitude along rivers (Mullinger et al., 2007, 2009; Cook, 2013). We used four different end-member activities in our simulations to account for the spatial heterogeneity in groundwater ^{222}Rn activities. Cook (2013) shows that the sensitivity toward the end-member activity is especially high when the ratio of groundwater activity to river water activity is low. In the Mähringsbach catchment, the mean activity of all end-member samples was 84,050 Bqm^{-3}, while the mean stream water activity was 1,743 Bqm^{-3}. This high gradient let us believe that the sensitivity toward the end-member activity did not lead to significant errors in calculated groundwater fluxes.

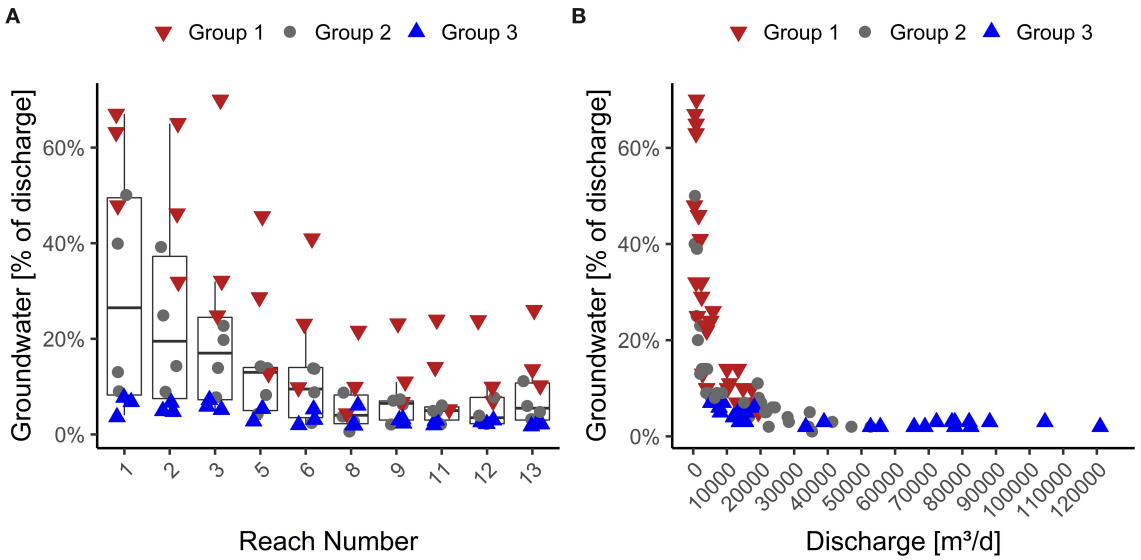

FIGURE 6 | Left **(A)** Variation of groundwater inflow in % of the total discharge in the measurement period for each reach. Right **(B)** Groundwater inflow in % of the total discharge over discharge for the reach.

Degassing is a second significant uncertainty for the ^{222}Rn mass balance. Using the FINIFLUX model, degassing was not measured but calculated using river width, depth, and flow velocity. Frei and Gilfedder (2015) suggest that this is only a problem for very turbulent conditions such as rapids and waterfalls that deviate significantly from the systems for which the empirical degassing equations were derived. The Mähringsbach catchment has an average slope of 0.6%, and its flow has relatively low turbulence, thus we do not believe there are major errors in calculated groundwater fluxes due to parameterization of degassing.

To assess how the degassing coefficient (k in equation 1) and the groundwater end-member (c_{gw} and k in Equation 1) quantitatively influence groundwater discharge, we calculated the cumulative groundwater flux for two scenarios (March 19, 2019, with the highest and with July 13, 2020, the lowest discharge) with changed values of both parameters. We changed the ^{222}Rn end-member activity and the degassing by 25% (**Figure 7**). The cumulative groundwater flux was used to show how the uncertainty in k and C_{gw} affect model results (**Figure 7**). The modeled cumulative groundwater flux at the end of the stream for March 19, 2019, was 2,780 m^3 d^{-1}, while for July 13, 2020, it was 1,820 m^3d^{-1}. With the groundwater end-member activity reduced by 25%, the modeled cumulative groundwater flux increased by 39% for March 19, 2019, and 43% for July 13, 2020, respectively. With increased groundwater end-member activity (by 25%), the modeled values were reduced by 28% and 17% for the same two sampling campaigns. While both scenarios reacted similarly to the increase in end-member activity, the low flow situation appeared to be less affected by a decrease in the end-member activity. Increasing the degassing coefficient by 25% increased the cumulative groundwater flux by 35% for March 19, 2019, and 24% for July 13, 2020, respectively. Decreasing the degassing coefficient by 25% decreased the modeled value by 35 and 22% for the same measurement dates. This shows that higher groundwater fluxes are more sensitive to ^{222}Rn end-member activity and degassing than the low groundwater fluxes. It also shows that the mass balance is highly sensitive to the degassing parameter k, with a similar sensitivity to the groundwater end-member. This fits a sensitivity analysis conducted by Cartwright and Gilfedder (2015), where a variation of k by −25% reduced the groundwater inflow by 25–30%. On the other hand, a variation of by +25% increased the groundwater inflow by 28%.

As in all ^{222}Rn mass balance models, losing conditions cannot be assessed in FINIFLUX as the model analyses the change in concentration rather than the change in mass between two points along the stream. Therefore, we cannot be sure if reaches with near-zero groundwater flux are actually losing reaches.

Groundwater Inflow

A spatial and temporal shift in groundwater inflow was observed along the Mähringsbach stream over the sampling period. Peaks in Groundwater inflow were located in the first two reaches and in the ninth reach. Their proximity to a groundwater-fed wetland can explain the high groundwater inflow rates in the upper two reaches (**Figure 5**). The fen provides a consistent groundwater flux leading to a high proportion of groundwater in steam water when discharge is low. In reaches 3 and 5, we observe very low groundwater inflow rates, which we assume is due to the poor connection with the aquifer. We also observed bedrock directly below the stream's sediments when collecting samples for the groundwater end-member estimation. Reach 6 runs through the city of Rehau, where the stream has been extensively channelized, with the riverbed being concreted at some locations, inhibiting groundwater-surface-water exchange (**Figure 5**). We found additional peaks in groundwater influx

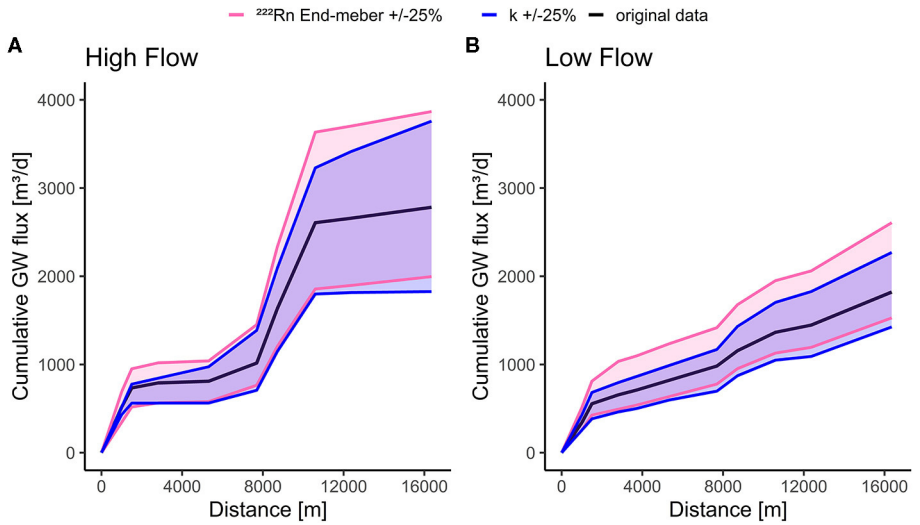

FIGURE 7 | Sensitivity of the mass-balance model to the groundwater end-member and degassing co-efficient k. The ^{222}Rn end-member activity and k were varied by ±25% for cumulative groundwater flux for time periods with the highest discharge (March 19, 2019) **(A)** and lowest (July 13, 2020) **(B)** discharge.

in the reaches 8 and 9. They are located at a break of slope in the landscape (**Figure 5**), meaning there is a rapid decrease in streambed slope, changing the streambed slope from 0.6 to 0.2%. Since we only measured the topographical height of the streambed at our measurement points, we assume the higher groundwater inflow to reach 8 to indicate that the break of the slope is located in reach 8. Cartwright et al. (2014) found similar patterns in the King River in Australia. This topographical control of groundwater inflow is also discussed in Sophocleous (2002) as a hinge line in the landscape that leads to groundwater upwelling. In the last three reaches, the river flows through a flat landscape where groundwater contributions are low because the hydrological gradient is small.

Groundwater inflow to the Mähringsbach increases with increasing discharge. Similar results were found in Australian rivers (Cartwright et al., 2014; Cartwright and Gilfedder, 2015). They postulated that groundwater table and discharge increase due to periods of rainfall recharging the local aquifer. However, we could not find a correlation (<0.5) between precipitation, the actual precipitation index (API), defined as the sum of precipitation in the 7, 14, or 21 days prior to the measurement, and groundwater inflow. Despite this, we believe a similar mechanism is likely to apply in our study area but is less pronounced than in the highly seasonal semi-arid Australian landscape. This is likely due to differences in weather systems between Australia and Central Europe. Central Europe is dominated by western winds providing frequent, small precipitation events, while in Australia, a strong seasonality with a pronounced dry and wet season predominates.

Our results show that in contrast to the absolute groundwater flux, the proportion of groundwater declines with increasing discharge. We found this effect in all reaches (**Supplementary Figure 1**). For example, on March 13, 2019, the Mähringsbach had 0.6 m^3 d^{-1} m groundwater inflow but only 2% groundwater proportion in reach 9, while on July 13, 2020, reach 3 had 0.08 m^3 d^{-1} m inflow but 70% groundwater proportion. This is likely caused by active interflow and surface flow during wet conditions diluting the groundwater component. In this case, discharge increases faster than infiltration to the groundwater due to activation of short, radon-free flow paths such as overland flow from the wetland area. Other water sources, such as tributaries and drains, which are more abundant and dominant downstream, are also likely to be important water sources not contributing to the groundwater proportion. Cartwright and Gilfedder (2015) found a similar pattern in their investigated Australian streams. Atkinson et al. (2015) found in a multi-tracer approach that the cumulative inflow of groundwater dropped from 25–46% during average conditions to 8–21% during flood periods.

In contrast, Brown et al. (2007) found that groundwater proportion of up to 65% but increased with increasing discharge at three sites in an alpine stream. This could be due to different hydrological responses in steep alpine catchments. Different water sources, such as snowmelt that are not present in Australian streams, are less important for the Mähringsbach due to its low altitude and sporadic snow cover in winter. Cartwright and Gilfedder (2015) showed that groundwater is an important, if not the sole component of river water in the headwater, but not so important once the stream became larger. We observed a similar pattern in the Mähringsbach.

Ecological Implications

A change from perennial to intermit flow can result from climate change, water abstraction, and alteration and intensification of land use (Bruno et al., 2020). This decline in permeant flow leads to a loss of ecosystem services (Ward et al., 2020). Ward et al. (2020) predicted a disconnection of the headwater's flow pathways in Oregon by up to 25% during the driest months,

which leads to a decrease in flowing river network length. Groundwater is a significant water reservoir that is not rapidly influenced by dry periods. Therefore, it can function as a buffer against short-term extremes in hydrological dynamics. We did not observe a disconnection of the river during drought, but we found that the proportion of groundwater in discharge exceeded 70% during drought conditions. Since groundwater is the last available water source during drought, river disconnection might become a problem in central European lower mountain ranges by either more extreme events than studied here or by compounding drought conditions over a number of years. During our sampling period, additional water was pumped into the stream by the Bavarian State in July 2019 to prevent the stream from drying out and, subsequently, preserve the critical habitat for the freshwater pearl mussel. This highlights the importance of consistent flow in this headwater stream but is unlikely to be a long-term solution to water scarcity.

The plant communities of small streams and riparian wetlands have a high biodiversity compared to drier habitats but are especially threatened by the changes in hydrology due to climate change (Dwire et al., 2018). Besides the effect of groundwater on the stream (i.e., sustaining streamflow during drought and change in water chemistry), it also affects the river bank and surrounding riparian area (Beatty et al., 2018). Riparian vegetation provides shade, which leads to declining evaporation rates and buffers temperature extremes (Beatty et al., 2018). Shade provides a valuable service helping to maintain streamflow and cool water temperatures, which is essential for a range of stream biota. This can be seen as contributing to improved resilience of the stream and its surrounding ecosystem, as well as contributing to maintaining the habitat requirements of aquatic species.

In addition to the threat of river disconnection, groundwater and surface water may differ significantly in their chemical and physical properties (e.g., nutrients, temperature, and metals such as Fe and Mn). This change of properties could lead to a shift in fauna and flora composition of the streams prior to stream disconnection. The effect of groundwater contribution to stream ecosystems is diverse and complex and can vary over time (**Figure 6**). The variation in the groundwater contribution along the downstream reaches of the Mähringsbach are relatively small (5–20%), while reaches 1 and 2 show a considerable variation (5–70%). These reaches are fed continuously by groundwater since the Mähringbach originates from a groundwater-fed bog and flows through riparian wetlands. Lowry et al. (2007) could show that zones of groundwater inflow in wetlands don't change spatially over time. This also highlights the importance of riparian wetlands for the hydrology of watersheds reviewed in Acreman and Holden (2013).

We could show that in times of drought, groundwater flux can prevent the stream from becoming ephemeral. Datry et al. (2007) showed that the diversity and density of hyporheic invertebrate in the Selwyn River, New Zealand increases with flow permanence. A 30–40% higher taxon richness of hyporheic invertebrates was found at groundwater-dominated sites (Datry et al., 2007). On the other hand, Brown et al. (2007) showed that only 1 of 20 of the predominant macroinvertebrate taxa in the Taillon-Gabiétous basin had their optimum when groundwater flux contributed >50% to the discharge. These studies show that invertebrate communities react to both flow permanence and changes in the groundwater surface water ratio.

Power et al. (1999) suggest that groundwater inflow is crucial for fish populations because it buffers hot summer and cold winter temperatures and moderates short-term temperature fluctuations in fish breeding sites. Beatty et al. (2018) were able to relate freshwater cobbler's upstream movement (*Tandanus bostocki*) to discharge and the proportion of groundwater in discharge. River disconnection during drought inhibits the migration of fish in headwaters. Since freshwater pearl mussels have a parasitic phase in their life cycle (glochidia live on the gills of trout), their survival depends on host fish populations (Geist, 2010). Groundwater flux may prevent river disconnection, but the effects of hydrological processes on the habitat of juvenile mussels, which stay up to 5 years in the hyporheic zone, are poorly understood (Geist, 2010). For the conservation of this species, it will be essential to understand how the groundwater flux influences the growth and survival of juvenile mussels.

As the mixing zone of groundwater and surface water, the hyporheic zone functions as an important refuge for many aquatic species during droughts with low flow or even intermittent flow (Bruno et al., 2020). Such a refuge can be the source of recolonization and therefore increases the ecosystem's resilience to droughts.

CONCLUSION

Headwaters play an essential role in all catchments as they create both the basis for abiotic processes such as water flow and stream chemistry as well as form the beginning of the aquatic ecosystem in a river network. The complex interactions between hydrology, chemistry, and biology in headwater ecosystems are not sufficiently understood yet to develop scientifically-based management strategies for water management, nature conservation, and ecological restoration. One crucial aspect is the quantification of groundwater and spring water contribution during seasonal fluctuations.

Given the current climate change projections, it is specifically crucial to understand the catchment response to periods of drought, which are likely to increase in frequency and magnitude in the future. Headwater ecosystems are threatened by a lack of water as well as river disconnection from the groundwater, both of which influence the temperature regime and water chemistry if the origin of water sources changes significantly (in our case, from ∼10 to 70%). We have found that the groundwater inflow decreases during drought events and in summer in general. However, the proportion of groundwater that contributed to total streamflow increases during drought and is essential for the health and vitality of the ecosystem as it becomes the dominant water source. Groundwater is also a resource of economic interest with the potential for conflict between drinking water supplies and conservation. Hollering (2020) states in a regional study about wells in the Fichtel Mountains that spring ecosystems are especially endangered by drinking water abstraction.

Further research about groundwater inflow and its ecological impacts would allow obtaining interdisciplinary insight into a headwater's water quantity regulation and habitat quality. Appropriate management decisions can only be made when the impacts of prolonged dry spells on water quantity are well-understood. Stakeholders can develop, refine and apply management strategies to preserve groundwater resources as the last water source to keep rivers flowing in summer. This study provides evidence that a headwater's water management is of utmost importance to preserve important ecological habitats. Headwater preservation will decrease climate change impacts on our streams and freshwater ecosystems, providing essential ecosystem services, such as drinking and irrigation water supply and water purification, and reducing erosion.

DATA AVAILABILITY STATEMENT

The raw data supporting the conclusions of this article will be made available by the authors, without undue reservation.

AUTHOR CONTRIBUTIONS

RK and BG contributed to concept and study design, manuscript revision, read, and approved the submitted version. RK performed the data collection and analysis. BG was responsible for funding.

FUNDING

This work was supported by the Bavarian State Ministry of Science and the Arts in the Bavarian Climate Research Network (www.bayklif.de) as part of the AQUAKLIF project. This publication was funded by the German Research Foundation (DFG) and the University of Bayreuth in the funding program Open Access Publishing.

ACKNOWLEDGMENTS

We would like to thank our colleagues Lisa Kaule and Romy Wild for providing much helpful input and assisting in field measurements. Additionally, we thank Sven Frei for assisting in groundwater modeling, the Wasserwirtschaftsamt Hof (Bavaria) for granting permission to work in the catchment and providing data, and the Bavarian State Forest for permission to access the forest.

SUPPLEMENTARY MATERIAL

The Supplementary Material for this article can be found online at: https://www.frontiersin.org/articles/10.3389/frwa.2021.706932/full#supplementary-material

REFERENCES

Acreman, M., and Holden, J. (2013). How wetlands affect floods. *Wetlands* 33, 773–786. doi: 10.1007/s13157-013-0473-2

Alexander, R. B., Boyer, E. W., Smith, R. A., Schwarz, G. E., and Moore, R. B. (2007). The role of headwater streams in downstream water quality. *J. Am. Water Resour. Assoc.* 43, 41–59. doi: 10.1111/j.1752-1688.2007.00005.x

Allen, G. H., Pavelsky, T. M., Barefoot, E. A., Lamb, M. P., Butman, D., Tashie, A., et al. (2018). Similarity of stream width distributions across headwater systems. *Nat. Commun.* 9:610. doi: 10.1038/s41467-018-02991-w

Anibas, C., Tolche, A. D., Ghysels, G., Nossent, J., Schneidewind, U., Huysmans, M., et al. (2017). Delineation of spatial-temporal patterns of groundwater/surface-water interaction along a river reach (Aa River, Belgium) with transient thermal modeling. *Hydrogeol. J.* 26, 819–835. doi: 10.1007/s10040-017-1695-9

Atkinson, A. P., Cartwright, I., Gilfedder, B. S., Hofmann, H., Unland, N. P., Cendoelseófin, D. I., et al. (2015). A multi-tracer approach to quantifying groundwater inflows to an upland river; assessing the influence of variable groundwater chemistry. *Hydrol. Process.* 29, 1–12. doi: 10.1002/hyp.10122

Bartsch, S., Frei, S., Ruidisch, M., Shope, C. L., Peiffer, S., Kim, B., et al. (2014). River-aquifer exchange fluxes under monsoonal climate conditions. *J. Hydrol.* 509, 601–614. doi: 10.1016/j.jhydrol.2013.12.005

Bayerisches Landesamt für Umwelt (2017). *Niedrigwasser in Bayern*. Augsburg: Grundlagen, Veränderung und Auswirkungen.

Bayerisches Landesamt für Umwelt (2021). *Pegel Rehau/Schwesnitz.* Available online at: https://www.hnd.bayern.de/pegel/oberer_main_elbe/rehau-56122008/tabelle?methode=abfluss&begin=23.03.2020&end=25.03.2020 (accessed March 23, 2021).

Beatty, S. J., Morgan, D. L., McAleer, F. J., Ramsay, A. R., Yao, Y., Tian, Y., et al. (2018). Groundwater contribution to baseflow maintains habitat connectivity for *Tandanus bostocki* (*Teleostei: Plotosidae*) in a south-western Australian river. Role of groundwater in the dryland ecohydrological system: a case study of the heihe river basin. *Ecol. Freshw. Fish* 123, 6760–6776. doi: 10.1111/j.1600-0633.2010.00440.x

Bennett, K. E., Werner, A. T., and Schnorbus, M. (2012). Uncertainties in hydrologic and climate change impact analyses in headwater basins of British Columbia. *J. Clim.* 25, 5711–5730. doi: 10.1175/JCLI-D-11-00417.1

Blöschl, G., Hall, J., Parajka, J., Perdigão, R. A. P., Merz, B., Arheimer, B., et al. (2017). Changing climate shifts timing of European floods. *Science* 357, 588–590. doi: 10.1126/science.aan2506

Boulton, A. J., Findlay, S., Marmonier, P., Stanley, E. H., and Valett, H. M. (1998). The functional significance of the hyporheic zone in streams and rivers. *Annu. Rev. Ecol. Syst.* 29, 59–81. doi: 10.1146/annurev.ecolsys.29.1.59

Bourke, S. A., Cook, P. G., Shanafield, M., Dogramaci, S., and Clark, J. F. (2014). Characterisation of hyporheic exchange in a losing stream using radon-222. *J. Hydrol.* 519, 94–105. doi: 10.1016/j.jhydrol.2014.06.057

Brown, L. E., Milner, A. M., and Hannah, D. M. (2007). Groundwater influence on alpine stream ecosystems. *Freshw. Biol.* 52, 878–890. doi: 10.1111/j.1365-2427.2007.01739.x

Bruno, M. C., Doretto, A., Boano, F., Ridolfi, L., and Fenoglio, S. (2020). Role of the hyporheic zone in increasing the resilience of mountain streams facing intermittency. *Water* 12:2034. doi: 10.3390/w12072034

Burnett, W. C., and Dulaiova, H. (2006). Radon as a tracer of submarine groundwater discharge into a boat basin in Donnalucata, Sicily. *Cont. Shelf Res.* 26, 862–873. doi: 10.1016/j.csr.2005.12.003

Cardenas, M. B., Ford, A. E., Kaufman, M. H., Kessler, A. J., and Cook, P. L. M. (2016). Hyporheic flow and dissolved oxygen distribution in fish nests: The effects of open channel velocity, permeability patterns, groundwater upwelling. *J. Geophys. Res. Biogeosci.* 121, 3113–3130. doi: 10.1002/2016JG003381

Cartwright, I., and Gilfedder, B. (2015). Mapping and quantifying groundwater inflows to deep creek (maribyrnong catchment, SE Australia) using 222Rn, implications for protecting groundwater-dependant ecosystems. *Appl. Geochem.* 52, 118–129. doi: 10.1016/j.apgeochem.2014.11.020

Cartwright, I., Hofmann, H., Gilfedder, B., and Smyth, B. (2014). Understanding parafluvial exchange and degassing to better quantify groundwater inflows using 222Rn: the King river, southeast Australia. *Chem. Geol.* 380, 48–60. doi: 10.1016/j.chemgeo.2014.04.009

Cartwright, I., Hofmann, H., Sirianos, M. A., Weaver, T. R., and Simmons, C. T. (2011). Geochemical and 222Rn constraints on baseflow to the Murray river, Australia, and timescales for the decay of low-salinity groundwater lenses. *J. Hydrol.* 405, 333–343. doi: 10.1016/j.jhydrol.2011.05.030

Constantz, J. (2008). Heat as a tracer to determine streambed water exchanges. *Water Resour. Res.* 44. doi: 10.1029/2008WR006996

Cook, P. G. (2013). Estimating groundwater discharge to rivers from river chemistry surveys. *Hydrol. Process.* 27, 3694–3707. doi: 10.1002/hyp.9493

Cook, P. G., Wood, C., White, T., Simmons, C. T., Fass, T., and Brunner, P. (2008). Groundwater inflow to a shallow, poorly-mixed wetland estimated from a mass balance of radon. *J. Hydrol.* 354, 213–226. doi: 10.1016/j.jhydrol.2008.03.016

Corbett, D., Burnett, W., Cable, P., and Clark, S. (2006). A multiple approach to the determination of radon fluxes from sediments. *J. Radioanal. Nucl. Chem.* 236, 247–253. doi: 10.1007/BF02386351

Cranswick, R. H., Cook, P. G., and Lamontagne, S. (2014). Hyporheic zone exchange fluxes and residence times inferred from riverbed temperature and radon data. *J. Hydrol.* 519, 1870–1881. doi: 10.1016/j.jhydrol.2014.09.059

Datry, T., Larned, S. T., and Scarsbrook, M. R. (2007). Responses of hyporheic invertebrate assemblages to large-scale variation in flow permanence and surface subsurface exchange. *Freshw. Biol.* 52, 1452–1462. doi: 10.1111/j.1365-2427.2007.01775.x

Denic, M., and Geist, J. (2017). The freshwater pearl mussel *Margaritifera margaritifera* in Bavaria, Germany—population status, conservation efforts and challenges. *Biol. Bull.* 44, 61–66. doi: 10.1134/S1062359017010034

Doherty, J. E., Hunt, R. J., and Tonkin, M. J. (2010). Approaches to highly parameterized inversion: a guide to using PEST for model-parameter and predictive-uncertainty analysis. *US Geol. Survey Sci. Invest. Rep.* 5211:71. doi: 10.3133/sir20105211

Downing, J. (2012). Global abundance and size distribution of streams and rivers. *Inland Waters* 2, 229–236. doi: 10.5268/IW-2.4.502

DWD (2021). *CDC - Climate Data Center*. Available online at: https://opendata.dwd.de/climate_environment/CDC/observations_germany/climate/monthly/more_precip/historical/ (accessed June 09, 2021).

Dwire, K. A., Mellmann-Brown, S., and Gurrieri, J. T. (2018). Potential effects of climate change on riparian areas, wetlands, and groundwater-dependent ecosystems in the Blue Mountains, Oregon, USA. *Clim. Serv.* 10, 44–52. doi: 10.1016/j.cliser.2017.10.002

Frei, S., Durejka, S., Le Lay, H., Thomas, Z., and Gilfedder, B. S. (2019). Quantification of hyporheic nitrate removal at the reach scale: exposure times versus residence times. *Water Resour. Res.* 55, 9808–9825. doi: 10.1029/2019WR025540

Frei, S., and Gilfedder, B. S. (2015). FINIFLUX: an implicit finite element model for quantification of groundwater fluxes and hyporheic exchange in streams and rivers using radon. *Water Resour. Res.* 51, 6776–6786. doi: 10.1002/2015WR017212

Geist, J. (2010). Strategies for the conservation of endangered freshwater pearl mussels (*Margaritifera margaritifera* L.): a synthesis of conservation genetics and ecology. *Hydrobiologia* 644, 69–88. doi: 10.1007/s10750-010-0190-2

German Meteorological Society (2021). *Wetter und Klima - Deutscher Wetterdienst - CDC (Climate Data Center)*. Available online at: https://www.dwd.de/DE/klimaumwelt/cdc/cdc_node.html (accessed March 03, 2021).

Gilfedder, B. S., Cartwright, I., Hofmann, H., and Frei, S. (2019). Explicit modeling of radon-222 in hydrogeosphere during steady state and dynamic transient storage. *Groundwater* 57, 36–47. doi: 10.1111/gwat.12847

Gomi, T., Sidle, R. C., and Richardson, J. S. (2002). Understanding processes and downstream linkages of headwater systemsheadwaters differ from downstream reaches by their close coupling to hillslope processes, more temporal and spatial variation, and their need for different means of protection from land use. *Bioscience* 52, 905–916. doi: 10.1641/0006-3568(2002)052[0905:UPADLO]2.0.CO;2

Hancock, P. J., Boulton, A. J., and Humphreys, W. F. (2005). Aquifers and hyporheic zones: towards an ecological understanding of groundwater. *Hydrogeol. J.* 13, 98–111. doi: 10.1007/s10040-004-0421-6

Harder, P., Pomeroy, J. W., and Westbrook, C. J. (2015). Hydrological Resilience of a canadian rockies headwaters basin subject to changing climate, extreme weather, and forest management. *Hydrol. Process.* 29, 3905–3924. doi: 10.1002/hyp.10596

Hatch, C. E., Fisher, A. T., Revenaugh, J. S., Constantz, J., and Ruehl, C. (2006). Quantifying surface water groundwater interactions using time series analysis of streambed thermal records: method development. *Water Resour. Res.* 42. doi: 10.1029/2005WR004787

Hollering, W. (2020). *Meesia triquetra*, *Carex loliacea*, *Carex heleonastes* sowie weitere außergewöhnliche funde von reliktarten in zwei quellmooren im fichtelgebirge. *Hoppea Denkschrif. Regensburg. Botan. Gesellschaft* 81, 159–172.

Huang, S., Krysanova, V., and Hattermann, F. (2015). Projections of climate change impacts on floods and droughts in Germany using an ensemble of climate change scenarios. *Reg. Environ. Change* 15, 461–473. doi: 10.1007/s10113-014-0606-z

IPCC (2014). *Climate Change 2014: Synthesis Report. Contribution of Working Groups I, II and III to the Firth Assessment Report of the Intergovernmental Panel on Climate Change*. Geneva: IPCC.

IPCC (2018). "Annex I: Glossary [Matthews, J.B.R. (ed.)]," in Global Warming of 1.5°C. An IPCC Special Report on the Impacts of Global Warming of 1.5°C Above Pre-industrial Levels and Related Global Greenhouse Gas Emission Pathways, in the Context of Strengthening the Global Response to the Threat of Climate Change, Sustainable Development, and Efforts to Eradicate Poverty, eds V. Masson-Delmotte, P. Zhai, H.-O. Pörtner, D. Roberts, J. Skea, P. R. Shukla, A. Pirani, W. Moufouma-Okia, C. Péan, R. Pidcock, S. Connors, J. B. R. Matthews, Y. Chen, X. Zhou, M. I. Gomis, E. Lonnoy, T. Maycock, M. Tignor, and T. Waterfield.

Kaufman, M. H., Cardenas, M. B., Buttles, J., Kessler, A. J., and Cook, P. L. M. (2017). Hyporheic hot moments: Dissolved oxygen dynamics in the hyporheic zone in response to surface flow perturbations. *Water Resour. Res.* 53, 6642–6662. doi: 10.1002/2016WR020296

Kawanishi, R., Inoue, M., Dohi, R., Fujii, A., and Miyake, Y. (2013). The role of the hyporheic zone for a benthic fish in an intermittent river: a refuge, not a graveyard. *Aquat. Sci.* 75, 425–431. doi: 10.1007/s00027-013-0289-4

Keery, J., Binley, A., Crook, N., and Smith, J. W. N. (2007). Temporal and spatial variability of groundwater–surface water fluxes: development and application of an analytical method using temperature time series. *J. Hydrol.* 336, 1–16. doi: 10.1016/j.jhydrol.2006.12.003

Kingston, D. G., and Taylor, R. G. (2010). Sources of uncertainty in climate change impacts on river discharge and groundwater in a headwater catchment of the Upper Nile Basin, Uganda. *Hydrol. Earth Syst. Sci.* 14, 1297–1308. doi: 10.5194/hess-14-1297-2010

Kreps, H. (1954). Näherungsverfahren bei hydrometrischen Feldarbeiten und ihrer Auswertung. *Österreichi. Wasserwirtsch.* 6, 60–65.

Lamontagne, S., and Cook, P. G. (2007). Estimation of hyporheic water residence time in situ using 222Rn disequilibrium. *Limnol. Oceanogra. Methods* 5, 407–416. doi: 10.4319/lom.2007.5.407

Lee, J.-M., and Kim, G. (2006). A simple and rapid method for analyzing radon in coastal and ground waters using a radon-in-air monitor. *J. Environ. Radioact.* 89, 219–228. doi: 10.1016/j.jenvrad.2006.05.006

Lowry, C. S., Walker, J. F., Hunt, R. J., and Anderson, M. P. (2007). Identifying spatial variability of groundwater discharge in a wetland stream using a distributed temperature sensor. *Water Resour. Res.* 43. doi: 10.1029/2007WR006145

Luce, C., Staab, B., Kramer, M., Wenger, S., Isaak, D., and McConnell, C. (2014). Sensitivity of summer stream temperatures to climate variability in the Pacific Northwest. *Water Resour. Res.* 50, 3428–3443. doi: 10.1002/2013WR014329

Malcolm, I. A., Youngson, A. F., and Soulsby, C. (2003). Survival of salmonid eggs in a degraded gravel-bed stream: effects of groundwater-surface water interactions. *River Res. Appl.* 19, 303–316. doi: 10.1002/rra.706

McCallum, J. L., Cook, P. G., Berhane, D., Rumpf, C. , and McMahon, G. A. (2012). Quantifying groundwater flows to streams using differential flow gaugings and water chemistry. *J. Hydrol.* 416–417, 118–132.

Mullinger, N. J., Binley, A. M., Pates, J. M., and Crook, N. P. (2007). Radon in Chalk streams: Spatial and temporal variation of groundwater sources in the Pang and Lambourn catchments, UK. *J. Hydrol.* 339, 172–182.

Mullinger, N. J., Pates, J. M., Binley, A. M., and Crook, N. P. (2009). Controls on the spatial and temporal variability of 222Rn in riparian groundwater in

a lowland Chalk catchment. *J. Hydrol.* 376, 58–69. doi: 10.1016/j.jhydrol.2009.07.015

O'Connor, D. J., and Dobbins, W. E. (1958). Mechanism of reaeration in natural streams. *Trans. Am. Soc. Civil Eng.* 123, 641–666. doi: 10.1061/TACEAT.0007609

Pittroff, M., Frei, S., and Gilfedder, B. S. (2017). Quantifying nitrate and oxygen reduction rates in the hyporheic zone using 222Rn to upscale biogeochemical turnover in rivers. *Water Resour. Res.* 53, 563–579. doi: 10.1002/2016WR018917

Power, G., Brown, R. S., and Imhof, J. G. (1999). Groundwater and fish—insights from northern North America. *Hydrol. Process.* 13, 401–422. doi: 10.1002/(SICI)1099-1085(19990228)13:3<401::AID-HYP746>3.0.CO;2-A

Schubert, M., Siebert, C., Knoeller, K., Roediger, T., Schmidt, A., and Gilfedder, B. (2020). Investigating groundwater discharge into a major river under low flow conditions based on a radon mass balance supported by tritium data. *Water* 12:2838. doi: 10.3390/w12102838

Sophocleous, M. (2002). Interactions between groundwater and surface water: the state of the science. *Hydrogeology J.* 10, 52–67. doi: 10.1007/s10040-001-0170-8

Sternecker, K., Cowley, D. E., and Geist, J. (2013). Factors influencing the success of salmonid egg development in river substratum. *Ecol. Freshw. Fish* 22, 322–333. doi: 10.1111/eff.12020

Unland, N. P., Cartwright, I., Andersen, M. S., Rau, G. C., Reed, J., Gilfedder, B. S., et al. (2013). Investigating the spatio-temporal variability in groundwater and surface water interactions: a multi-technique approach. *Hydrol. Earth Syst. Sci.* 17, 3437–3453. doi: 10.5194/hess-17-3437-2013

van Loon, A. F. (2013). *On the Propagation of Drought: How Climate and Catchment Characteristics Influence Hydrological Drought Development and Recovery* (Ph.D. thesis). Research@WUR, Wageningen University, Wageningen, Netherlands, 198.

Ward, A. S., Wondzell, S. M., Schmadel, N. M., and Herzog, S. P. (2020). Climate change causes river network contraction and disconnection in the H.J. Andrews experimental forest, Oregon, USA. *Front. Water* 2:7. doi: 10.3389/frwa.2020.00007

Zerbisch, M., Grothmann, T., Schroeter, D., Hasse, C., Fritsch, U., and Cramer, W. (2005). *Klimawandel in Deutschland*. Dessau: Vulnerabilität und Anpassungsstrategien klimasensitiver Systeme.

Zhou, S., Yuan, X., Peng, S., Yue, J., Wang, X., Liu, H., et al. (2014). Groundwater-surface water interactions in the hyporheic zone under climate change scenarios. *Environ. Sci. Pollut. Res.* 21, 13943–13955. doi: 10.1007/s11356-014-3255-3

Conflict of Interest: The authors declare that the research was conducted in the absence of any commercial or financial relationships that could be construed as a potential conflict of interest.

Publisher's Note: All claims expressed in this article are solely those of the authors and do not necessarily represent those of their affiliated organizations, or those of the publisher, the editors and the reviewers. Any product that may be evaluated in this article, or claim that may be made by its manufacturer, is not guaranteed or endorsed by the publisher.